Available online at www.sciencedirect.com
SCIENCE DIRECT®
Journal of Solid State Chemistry 178 (2005) 825–830
JOURNAL OF SOLID STATE CHEMISTRY
www.elsevier.com/locate/jssc

Hydrothermal synthesis and luminescence behavior of rare-earth-doped $NaLa(WO_4)_2$ powders

Feng Wang, Xianping Fan*, Daibo Pi, Zhiyu Wang, Minquan Wang

Institute of Inorganic Materials, Department of Materials Science and Engineering, Zhejiang University, No. 38, Zheda Road, Hangzhou City, Zhejiang province 310027, PR China

Received 8 November 2004; received in revised form 30 December 2004; accepted 2 January 2005

Abstract

$NaLa(WO_4)_2$ powders doped with Eu^{3+}, Nd^{3+}, and Er^{3+} have been synthesized by a mild hydrothermal method and a crystal of exclusive scheelite phase could be obtained at low temperature. From the spectrum of Eu^{3+} it has been concluded that the dopant Eu^{3+} ion occupies a La^{3+} site and mainly takes the site with C_2 symmetry. The higher quenching concentration can be observed in the Eu^{3+}-doped $NaLa(WO_4)_2$ powders. The Er^{3+}- and Nd^{3+}-doped $NaLa(WO_4)_2$ powders exhibit luminescence in the near infrared (Er^{3+} at 1550 nm, and Nd^{3+} at 1060 nm). The transition mechanism of the up-conversion luminescence of the Er^{3+}-doped $NaLa(WO_4)_2$ powders can be ascribed to two photons absorption process.

Keywords: Hydrothermal synthesis; Rare-earth ions; Luminescence; Tungstate

1. Introduction

Double alkaline rare-earth molybdates and tungstates ($ARe(MO_4)_2$, where $A = K$, Na, $Re = La$, Y, and $M = Mo$, W) form a wide variety of inorganic compounds having tetragonal and monoclinic symmetries. The $ARe(MO_4)_2$ doped with trivalent rare earth (RE) and transition-metal activators has played an important role in quantum electronics for more than three decades [1]. Their structural diversity provides these crystals with numerous physical properties. In addition to the well-known laser potential [2,3], it is also possible to take benefit of the nonlinearities of the host as efficient Stokes converters of laser radiation [4–9]. These compounds have been prepared by several different processes such as the flux growth [10,11], solid-state reaction [12], and hydrothermal reaction over an extensive period [13].

It is well known that rare-earth-doped materials can find a wide variety of applications including phosphors for lighting, display, and X-ray imaging [14–16], scintillators [17], laser [3], and amplifiers for fiber-optic communication [18]. While over a long time the investigations on the $ARe(MO_4)_2$ family of compounds are concentrated on the single crystals to take advantage of the laser properties and compounds $ARe(MO_4)_2$ with small grain size, other uses have received little attention. Recently, it has been revealed that powder samples of this family might be promising candidates as phosphors for visual display [19] and solid-state lighting [20]. But the traditional synthesis method for prepared powder samples of $ARe(MO_4)_2$ is usually solid-state reaction over 800 °C, involving a complicated procedure and long reaction time.

Byrappa et al. [13] recently reported preparation of $NaLa(WO_4)_2$ single crystal via a complicated hydrothermal process that required long reaction time of several days. In this paper, a simple hydrothermal route to synthesis rare-earth-doped luminescent $NaLa(WO_4)_2$ powders was developed and the luminescence behavior

*Corresponding author. Fax: +86 571 8795 1234.
E-mail address: fanxp@cmsce.zju.edu.cn (X. Fan).

0022-4596/$ - see front matter © 2005 Elsevier Inc. All rights reserved.
doi:10.1016/j.jssc.2005.01.001

of Eu^{3+}, Nd^{3+}, and Er^{3+} ions in $NaLa(WO_4)_2$ powders was described.

2. Experimental

Lanthanum chloride ($LaCl_3 \cdot 4H_2O$) and sodium tungstate ($Na_2WO_4 \cdot 2H_2O$) were used as raw materials. Europium chloride ($EuCl_3 \cdot nH_2O$), neodymium chloride ($NdCl_3 \cdot nH_2O$), and erbium chloride ($ErCl_3 \cdot nH_2O$) were prepared by dissolving corresponding rare-earth oxide (Eu_2O_3, Nd_2O_3, Er_2O_3) in dilute hydrochloric acid and then drying in order to remove the unreacted hydrochloric acid. Solution A was prepared by dissolving $LaCl_3 \cdot 4H_2O$ and $RECl_3 \cdot nH_2O$ ($RE = Eu^{3+}$, Nd^{3+}, and Er^{3+}) in 90 mL deionized water with the total metal cations being 3.6 mmol. The solution was then adjusted to the desired pH 6.0 with NaOH and stirred for 10 min at room temperature. Another solution B was prepared by dissolving 2.1375 g of $Na_2WO_4 \cdot 2H_2O$ (6.48 mmol) in 90 mL deionized water with initial pH 10.0 and stirred for 10 min at room temperature. Solution A was then added to solution B with vigorous magnetic stirring. The formed suspension was stirred continuously for 10 min and subsequently heated at 180 °C for 2 h in a Teflon-lined autoclave of 250 ml capacity with stirring. The white precipitate was separated by centrifugation and washed with deionized water and ethanol for several times. And then the precipitate was dried at 60 °C for 12 h and collected for characterization. For comparison, a sock of suspension was stirred under ambient pressure at room temperature for 2 h. The precipitate was washed and collected with the same procedure described above, which was referenced as as-precipitated sample.

The phase and crystallinity were analyzed by X-ray diffraction (XRD) (Philips XD98) using Cu$K\alpha$ radiation. Scanning electronic micrograph (SEM) was taken on a Philips XL 30. The excitation and emission spectra in the visible region were recorded on a HITACH F-4500 fluorescence spectrophotometer equipped with a Xe-arc lamp as excitation source. The luminescence decay curves were measured with a SP-750 monochromator, a PMT, a BOXCAR and an NCL multi-channel data collecting analysis system. The sample was excited by the emission line at 355 nm from the third harmonic of Xe-lamp pumped Q-switched Nd:YAG laser with pulse width of 25 ns and beam diameter of 1.5 mm. The pump repetition rate could be adjusted from single shot to 20 Hz. The emission spectra in the near-infrared region were recorded on a TRIAX550 monochromator (JOBIN YVON-SPEX) equipped with a PS/TC-1 detector (ELECTRO-OPTICAL SYSTEMS INC.). Two LDs of 800 and 980 nm were used as excitation source for Nd^{3+} ions and Er^{3+} ions, respectively. Up-conversion luminescent spectra were taken on the HITACH F-4500 fluorescence spectrophotometer with an external 980 nm LD as the excitation source, instead of the xenon source in the spectrophotometer. All measurements were performed at room temperature.

3. Results and discussion

Fig. 1 shows XRD patterns of the 5 mol% Eu^{3+}-doped samples obtained as-precipitated (A) and after hydrothermal treatment (B). Only a diffused broad trace can be found in the Fig. 1A, indicating that only amorphous $NaLa(WO_4)_2$ particles could be achieved at room temperature. After the sample was hydrothermal treated at 180 °C for 2 h in a Teflon-lined autoclave the XRD pattern shown in Fig. 1B exhibited prominent peaks well accordant with JCPDS standard card (79-1118) of tetragonal $NaLa(WO_4)_2$ crystal with no second phase. Obviously, the colloidal phase has completely crystallized during the hydrothermal synthesis. Fig. 2 shows the SEM photograph of the 5 mol% Eu^{3+}-doped $NaLa(WO_4)_2$ powders, which exhibit nearly spherical morphology. The particle diameter was found to be about 1–2 μm.

The Eu^{3+} ion is a good probe for the chemical environment of the rare-earth ion because probability of the $^5D_0 \rightarrow {}^7F_2$ transition (allowed by electric dipole) is very sensitive to relatively small changes in the surroundings, but the $^5D_0 \rightarrow {}^7F_1$ transition (allowed by magnetic dipole) is insensitive to the environment [21]. Thus, the ratio of the two intensities is a good measure for the symmetry of the Eu^{3+} site. In a site with inversion symmetry, the $^5D_0 \rightarrow {}^7F_1$ transition is dominating, while in a site without inversion symmetry, the $^5D_0 \rightarrow {}^7F_2$ transition is strongest [22]. In addition, the emitting level $^5D_0$ and the ground state $^7F_0$ are nondegenerate, and the $^5D_0 \rightarrow {}^7F_0$ emission can give

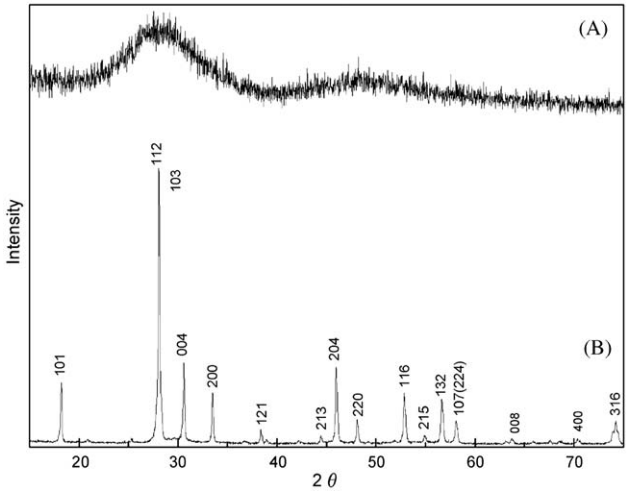

Fig. 1. XRD patterns of the 5 mol% Eu^{3+}-doped $NaLa(WO_4)_2$ powders (A) as precipitate, (B) after hydrothermal treatment.

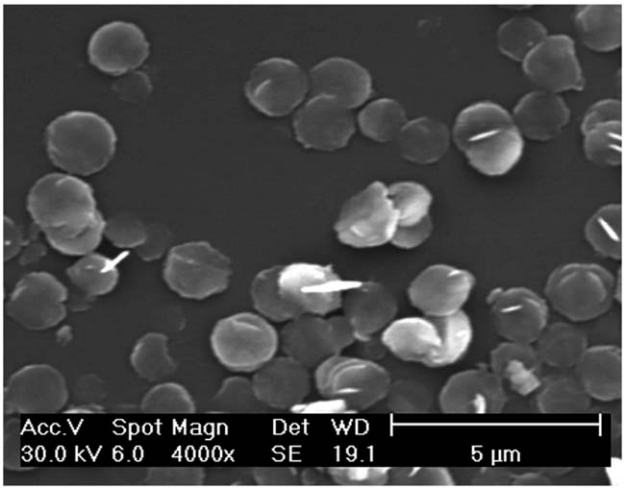

Fig. 2. SEM photograph of the 5 mol% Eu^{3+}-doped $NaLa(WO_4)_2$ powders.

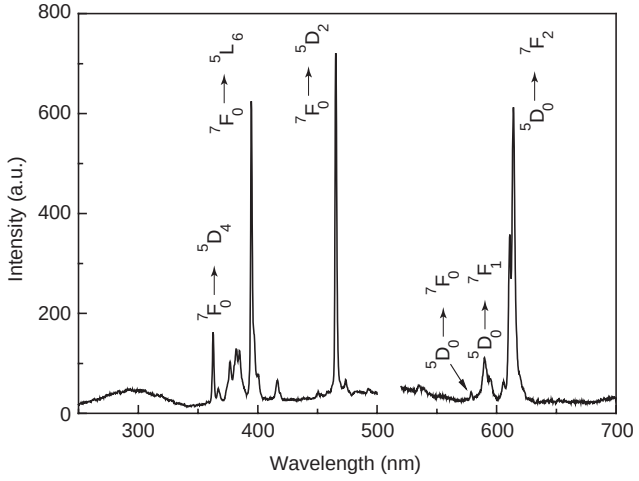

Fig. 3. Excitation (left, monitored at 614 nm) and emission (right, excited at 395 nm) spectra of the 5 mol% Eu^{3+}-doped $NaLa(WO_4)_2$ powders.

information about the impurity or if this ion occupies more than one site symmetry, particularly of the type C_{nv}, C_n, or C_s [23]. Fig. 3 shows the excitation (monitored at 614 nm) and emission (excited at 395 nm) spectra of the 5 mol% Eu^{3+}-doped $NaLa(WO_4)_2$ powders. The excitation spectrum shows a broad C–T (O→W) band along with sharp lines of Eu^{3+} ions at ~363 nm, ~395 nm, and ~465 nm ($^7F_0 \rightarrow {}^5D_4$, $^7F_0 \rightarrow {}^5L_6$, and $^7F_0 \rightarrow {}^5D_2$, respectively). The majority of the emission spectrum contains only the $^5D_0 \rightarrow {}^7F_J$ transitions, indicating that the higher levels were coupled to tungstate stretching vibrations and quenched by cross-relaxation. In addition, the $^5D_0 \rightarrow {}^7F_2$ intensity is about three times more than that of the $^5D_0 \rightarrow {}^7F_1$ transition, which is allowed even in the free ion case. The dominance of forced electric dipole transitions implies the loss of inversion symmetry of Eu^{3+} ions in the $NaLa(WO_4)_2$ powders, which is in accordance with the C_2 symmetry of the luminescent rare-earth ions in $KRe(WO_4)_2$ as determined by IR and Raman spectroscopy [24].

Fig. 4 shows that the ratio of $^5D_0 \rightarrow {}^7F_1$ to $^5D_0 \rightarrow {}^7F_2$ emission intensity is strongly dependent on excitation wavelength and doping concentration of Eu^{3+} ions. Similar correlation between the ratio of $^5D_0 \rightarrow {}^7F_1$ to $^5D_0 \rightarrow {}^7F_2$ emission intensity and excitation wavelength was also observed by Blasse et al. for compounds $K_9EuW_{10}O_{36} \cdot 18H_2O$ [25]. Blasse et al. attributed the phenomenon to the inhomogeneous composition of the samples and the diversity of penetration depth for different exciting radiation. It is well known that the compound $NaLa(WO_4)_2$ crystallizes in the tetragonal system of scheelite type with sodium and lanthanum disordered in the same site [26]. The symmetry of the RE site is D_{3d} with respect to all ions within the cell opened by the 12 nearest RE neighbor sites. The statistical

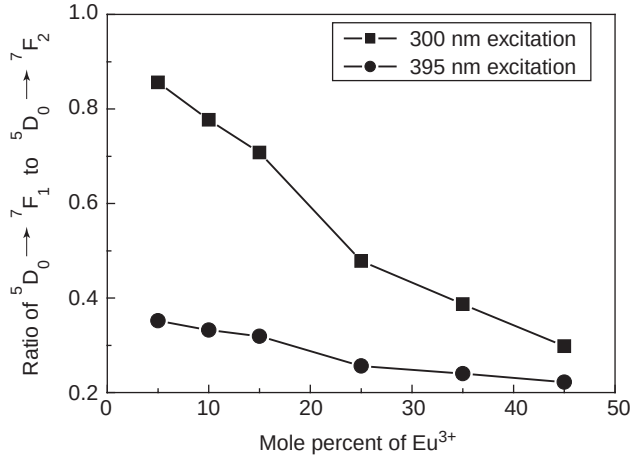

Fig. 4. Dependence of the ratio of $^5D_0 \rightarrow {}^7F_1$ to $^5D_0 \rightarrow {}^7F_2$ emission intensity under 300 and 395 nm excitation on mole percent of Eu^{3+} ions.

distribution of Na^+ and RE ions, however, will cause a reduction of the site symmetry D_{3d} and yield a set of D_{3d} subgroups (C_2, C_s, and C_1). Each subgroup of D_{3d} implies a special set of restrictions on the possible distribution of the Na^+ and RE ions [27]. Thus the variety in the ratio of $^5D_0 \rightarrow {}^7F_1$ to $^5D_0 \rightarrow {}^7F_2$ emission intensity under different exciting radiation can be concluded to be produced by two effects: (1) The Eu^{3+} ions have taken more than one site symmetries including D_{3d}. (2) Under C–T excitation (O→W, 300 nm), the Eu^{3+} located in the site symmetry D_{3d} could be excited more effectively. The decrease in the ratio of $^5D_0 \rightarrow {}^7F_1$ to $^5D_0 \rightarrow {}^7F_2$ emission intensity with increasing Eu^{3+} doping concentration reveals that the extent of deviation from D_{3d} symmetry was enhanced at higher doping concentration of Eu^{3+} ions.

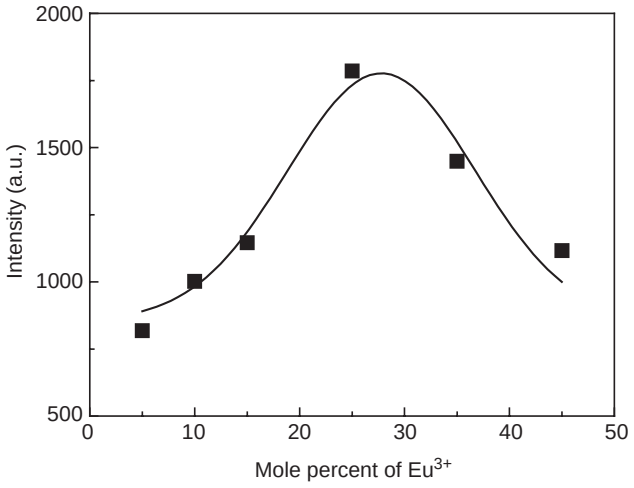

Fig. 5. Relationship between the luminescence intensity of the Eu^{3+}-doped $NaLa(WO_4)_2$ powders and mole percent of Eu^{3+} ions.

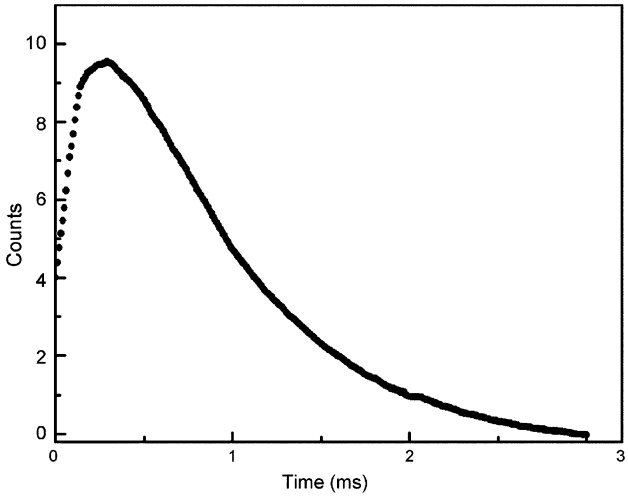

Fig. 6. Luminescence decay curve of the 5 mol% Eu^{3+}-doped $NaLa(WO_4)_2$ powders.

Fig. 5 shows the relationship between luminescence intensity of the $NaLa_{1-x}Eu_x(WO_4)_2$ powders by monitoring the emission of $^5D_0 \rightarrow {}^7F_2$ transition at 614 nm and doping concentration of Eu^{3+} ions. The higher concentration quenching can be observed. The concentration quenching can generally be attributed to the possible nonradiative transfer resulted from resonance energy transfer between neighboring rare-earth ions [28]. As described above, the $NaLa(WO_4)_2$ crystal adopts a sheelite-like tetragonal structure. The structure consists of WO_4 tetrahedron, NaO_8 and LaO_8 polyhedrons. LaO_8 polyhedrons are isolated from each other, with La^{3+} ions joined by means of La–O–W–O–La. This spatial arrangement will block resonance energy transfer between Eu^{3+} ions, which occupy the La^{3+} sites and result in higher luminescence concentration quenching. Therefore, the concentration quenching occurs at higher Eu^{3+} concentration in the $NaLa_{1-x}Eu_x(WO_4)_2$ powders. Thus, a desirable characteristic of the $NaLa_{1-x}Eu_x(WO_4)_2$ powders could obtained by doping more Eu^{3+} ions into the host $NaLa(WO_4)_2$ powders, which was of great benefit to their practical uses.

The luminescence decay curves of the $^5D_0$ state were obtained by monitoring the $^5D_0 \rightarrow {}^7F_2$ emission of Eu^{3+}. Fig. 6 shows the observed luminescence decay curves of the 5 mol% Eu^{3+}-doped $NaLa(WO_4)_2$ powders. The luminescence decay curve was approximately fitted to a single exponential, yielding the lifetimes of $\tau_{1/e} = 1.02$ ms. Fig. 7 shows the dependence of the $^5D_0$ excited-state lifetime of the Eu^{3+} in the $NaLa(WO_4)_2$ powders on the doping concentration of Eu^{3+} ions. The excited-state lifetime gradually increased with increasing doping concentration of Eu^{3+} ions and reached to a maximum at 25 mol% Eu^{3+} ions.

The same procedure was used to synthesize $NaLa(WO_4)_2$ powders doped with rare-earth ions that emit in

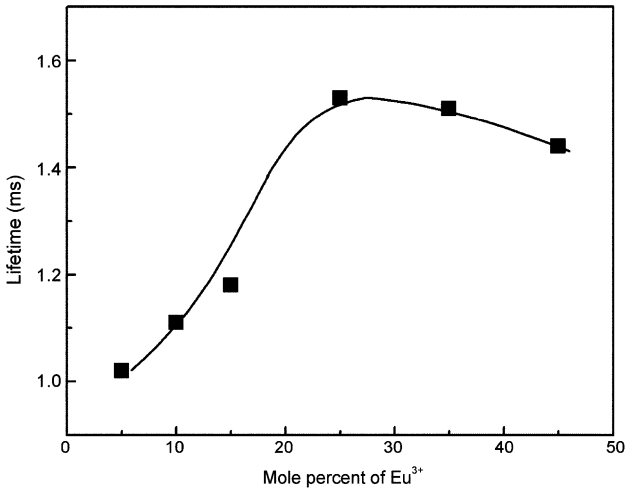

Fig. 7. Dependence of the $^5D_0$ excited-state lifetime of the Eu^{3+} in the $NaLa(WO_4)_2$ powders on mole percent of Eu^{3+} ions.

the near infrared. Fig. 8 shows the emission spectra in the near-infrared of the 5 mol% Er^{3+} (A, excited at 980 nm) and the 5 mol% Nd^{3+} (B, excited at 800 nm) doped $NaLa(WO_4)_2$ powders. The emission spectrum of the 5 mol% Nd^{3+}-doped $NaLa(WO_4)_2$ powders exhibits the typical Nd^{3+} transitions at 880, 1060, and 1330 nm ($^4F_{3/2} \rightarrow {}^4I_J$, $J = 9/2$, 11/2, and 13/2, respectively). The emission band of the 5 mol% Er^{3+}-doped $NaLa(WO_4)_2$ powders at 1550 nm can be attributed to $^4I_{13/2} \rightarrow {}^4I_{15/2}$ transition of Er^{3+}. The emission band of the Er^{3+} has obviously been split into four peaks (1509, 1540, 1562, and 1590 nm) in the 5 mol% Er^{3+}-doped $NaLa(WO_4)_2$ powders in comparison with the other Er^{3+}-doped materials [29,30]. It is because tungsten ions have high charge density due to their small size (0.41 nm [31]) and high charge (6+), which cause much polarization in the host material.

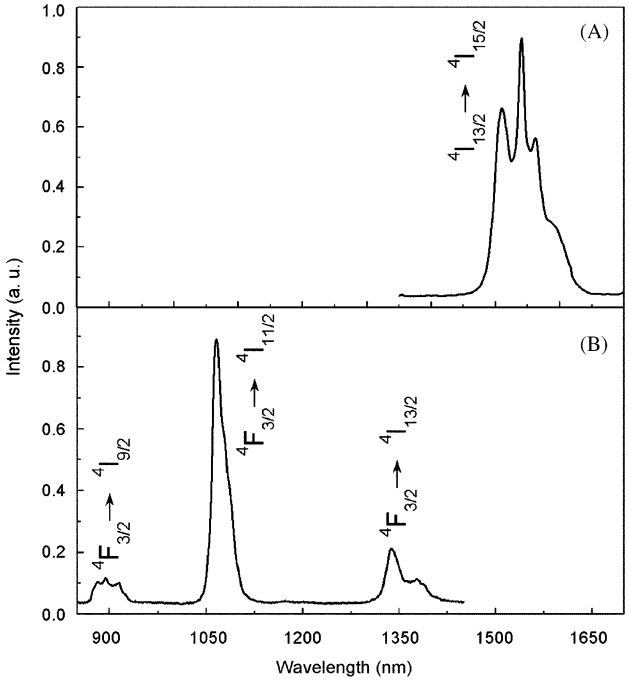

Fig. 8. Emission spectra in the near infrared of the 5 mol% Er^{3+} (A, excited at 980 nm) and the 5 mol% Nd^{3+} (B, excited at 800 nm) doped $NaLa(WO_4)_2$ powders.

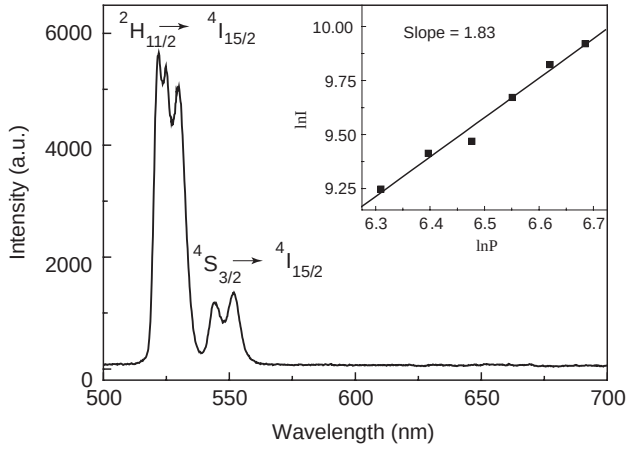

Fig. 9. Up-conversion luminescence spectrum of the 5 mol% Er^{3+} (excited at 980 nm)-doped $NaLa(WO_4)_2$ powders. Inset: Relationship between the up-conversion luminescence intensity and the pumping power of LD.

Fig. 9 shows the up-conversion luminescence of the 5 mol% Er^{3+}-doped $NaLa(WO_4)_2$ powders under 980 nm excitation. The strong green luminescence can be attributed to $^2H_{11/2} \rightarrow {}^4I_{15/2}$ (~525 nm) and $^4S_{3/2} \rightarrow {}^4I_{15/2}$ (~550 nm) transitions, respectively. Similar to emission band in the near infrared of Er^{3+}, the obvious splitting peaks of up-conversion luminescence can be observed. The inset of Fig. 9 shows the relationship between $\ln I$ and $\ln P$ where I is the up-conversion luminescence intensity (525 nm) and P the pumping power of LD. The slope can be found to be 1.83, which indicates that the up-conversion luminescence is due to a two-step excitation process: first excited from the ground state to the $^4I_{11/2}$ level by one photon absorption, and then excited to the $^4F_{7/2}$ level in large quantities by a second photon. The $^4S_{3/2}$ and $^2H_{11/2}$ levels are populated from $^4F_{7/2}$ level by multi-phonon relaxation, which resulted in luminescence corresponding to $^2H_{11/2} \rightarrow {}^4I_{15/2}$ and $^4S_{3/2} \rightarrow {}^4I_{15/2}$ transitions. This is accordance with the up-conversion mechanism of Er^{3+} ions which was described by sequential two-photon absorption or energy transfer up-conversion mechanisms [32–34]; both need the population in the $^4I_{11/2}$ level.

4. Conclusions

Rare-earth-doped $NaLa(WO_4)_2$ powders have been synthesized by a simple hydrothermal method. Well-crystallized scheelite phase could be obtained at low temperature. The dopant type and concentration can easily be varied. The higher luminescence quenching concentration can be observed in the Eu^{3+}-doped $NaLa(WO_4)_2$ powders. The Nd^{3+}- and Er^{3+}-doped $NaLa(WO_4)_2$ powders exhibit the typical emission spectra in the near infrared. The up-conversion luminescence of the Er^{3+}-doped $NaLa(WO_4)_2$ powders has also been observed and the transition mechanism of the up-conversion luminescence can be ascribed to two photons absorption process.

Acknowledgments

The authors gratefully acknowledge financial support for this research from the National Nature Science Foundation of China (No. 50472062, 50272059). The authors thank Lu Meihua of National University of Singapore for help with SEM photographs.

References

[1] A.A. Kaminskii, J.J. Eichler, K. Ueda, N.V. Klassen, B.S. Redkin, L.E. Li, J. Findeisen, D. Jaque, J. Garcia-Sole, J. Fernandez, R. Balda, Appl. Opt. 38 (21) (1999) 4533.
[2] M.J. Weber (Ed.), Handbook of Laser Science and Technology, vol. 1, CRC Press, Boca Raton, FL, 1982.
[3] A.A. Kaminskii, Crystalline Lasers: Physical Processes and Operating Schemes, CRC Press, Boca Raton, FL, 1996.
[4] V.A. Berenberg, S.N. Karpukhin, V.I. Mochalov, Sov. J. Quantum Electron. 17 (1987) 1178.
[5] V.S. Gulev, A.A. Pavlyuk, L.P. Kozeeva, V.F. Nesterenko, SPIE Solid State Lasers 1223 (1990) 103.
[6] C.J. Flood, D.R. Walker, H.M. van Driel, Appl. Phys. B 60 (1995) 309.

[7] A.A. Kaminskii, H.J. Eichler, D. Grebe, R. Macdonal, S.N. Bagaev, A.A. Pavlyuk, F.A. Kuznetsov, Phys. Status Solidi (a) 153 (1996) 281.
[8] A.A. Kaminskii, L. Li, A.V. Butashin, V.S. Mironov, A.A. Pavlyuk, S.N. Bagajev, K. Ueda, Opt. Rev. 4 (1997) 309.
[9] J.T. Murray, W.I. Austin, R.C. Powell, Advanced Solid State Lasers; Coeur d'Alen, Technical Digest, vol. 19, Optical Society of America, Washington DC, 1998, p. 249.
[10] G.F. Wang, Z.D. Luo, J. Cryst. Growth 102 (1990) 765.
[11] X.M. Han, G.F. Wang, J. Cryst. Growth 249 (2003) 167.
[12] Z.X. Cheng, Q.M. Lu, S.J. Zhang, J.H. Liu, X.J. Yi, F. Song, Y.F. Kong, J.R. Han, H.C. Chen, J. Cryst. Growth 222 (2001) 797.
[13] K. Byrappa, A. Jain, J. Mater. Res. 11 (11) (1996) 2869.
[14] C.R. Ronda, J. Lumin. 72–74 (1997) 49.
[15] T. Hase, T. Kano, E. Nakazawa, H. Yamamoto, Adv. Electronics Electron Phys. 79 (1990) 271.
[16] G. Blasse, Chem. Mater. 1 (1989) 294.
[17] G. Blasse, Chem. Mater. 6 (1994) 1465.
[18] D.B. Barber, C.R. Pollock, L.L. Beecroft, C.K. Ober, Opt. Lett. 22 (1997) 1247.
[19] Y.R. Do, Y.D. Huh, J. Electrochem. Soc. 147 (11) (2000) 4385.
[20] S. Neeraj, N. Kijima, A.K. Cheetham, Chem. Phys. Lett. 387 (2004) 2.
[21] P.P. Gawryszewska, M. Pietraszkiewicz, J.P. Richl, J. Legendziewicz, J. Alloys Comp. 300–301 (2000) 283.
[22] A.F. Kirby, F.S. Richardson, J. Phys. Chem. 87 (1983) 2544.
[23] C.A. Kodaira, H.F. Brito, O.L. Malta, O.A. Serra, J. Lumin. 101 (2003) 11.
[24] L. Macalik, J. Alloys Comp. 341 (2002) 226.
[25] G. Blasse, G.J. Dirksen, F. Zonnevijlle, Chem. Phys. Lett. 83 (3) (1981) 449.
[26] H.J. Li, G.Y. Hong, S.Y. Yue, J. Chinese Rare Earth Soc. 8 (1990) 37.
[27] G. Huber, W. Lenth, J. Lieberts, F. Lutz, J. Lumin. 16 (1978) 353.
[28] G. Blasse, J. Lumin. 1–2 (1970) 766.
[29] J.W. Stouwdam, F.C.J.M. van Veggel, Nano Lett. 2 (2002) 733.
[30] G.A. Kumar, R. Riman, S.C. Chae, Y.N. Jang, I.K. Bae, H.S. Moon, J. Appl. Phys. 95 (2004) 3243.
[31] R.D. Shannon, L.T. Prewitt, Acta Crystallogr. B 25 (1969) 925.
[32] J. Mendez-Rams, V. Lavin, I.R. Martin, J. Alloys. Comp. 323–324 (2001) 753.
[33] S. Tanabe, H. Hayashi, T. Hanada, Opt. Mater. 19 (2002) 343.
[34] F. Auzel, Chem. Rev. 104 (2004) 139.